

1 **Find the Food First: An Omnivorous Sensory Morphotype Predates Biomechanical**
2 **Specialization for Plant Based Diets in Phyllostomid Bats**

3

4 **Abstract**

5

6 The role of mechanical morphologies in the exploitation of novel niche space is well
7 characterized, however, the role of sensory structures in unlocking new niches is less clear. Here
8 we investigate the relationship between the evolution of sensory structures and diet during the
9 radiation of noctilionoid bats. With a broad range of foraging ecologies and a well-supported
10 phylogeny, noctilionoids constitute an ideal group for studying this relationship. We used
11 diffusible iodine-based contrast enhanced computed tomography (diceCT) scans of 44
12 noctilionoid species to analyze relationships between the relative volumes of three sensory
13 structures (olfactory bulbs, orbits, and cochleae) and diet. We found a positive relationship
14 between frugivory and both olfactory and orbit size. However, we also found a negative
15 relationship between nectarivory and cochlea size. Ancestral state estimates suggest that larger
16 orbits and olfactory bulbs were present in the common ancestor of family Phyllostomidae, but
17 not in other noctilionoid. This constellation of traits indicates a shift toward omnivory at the base
18 of Phyllostomidae, predating their radiation into an exceptionally broad range of dietary niches.
19 This is consistent with a scenario in which changes in sensory systems associated with foraging
20 and feeding set the stage for subsequent morphological modification and diversification.

21

22 **Keywords:** morphology, sensory, vision, olfaction, comparative analyses

23

24

25 **Introduction**

26

27 In the presence of ecological opportunity, novel morphological alterations can facilitate
28 the exploration and exploitation of new niches. Divergence within these new niches may result in
29 increased morphological disparity across lineages over time (Schluter 2000). Many studies of
30 such disparity have focused on skeletal elements of morphology that enhance fitness by
31 improving ecological performance (Herrel and Holanova 2008; Santana and Dumont 2009;
32 Arnold 2015; Grant and Grant 1993; Schluter and Price 1997) and morphological divergence in
33 response to diverse food types is a hallmark of well-studied radiations including those of
34 Darwin’s finches (Fyer and Iles 1972), cichlid fishes (Schluter 2000), and bats ((Freeman 2000;
35 Baker et al. 2012; Dumont et al. 2012; Santana et al. 2012; Hedrick and Dumont 2018) In the
36 limited cases in which sensory structures have been a focus of study within morphologically
37 disparate lineages, that focus has been directed to the role of sensory structures in sexual
38 selection, such as in sensory drive in cichlids (Seehausen et al. 2008), or in the context of
39 environmental change, as in the effects of climate on echolocation frequency (Jacobs et al.
40 2017). Literature on insect sensory structures have made great strides in using these sensory
41 systems to understand biochemical and neurological aspects of sensing (Beuhmann et al. 2020,
42 Martin et al. 2011). Researchers have even reached into the past to investigate the competitive
43 advantage of sightedness in trilobites (Henze and Oakley, 2015). Nevertheless, sensory structures
44 play key roles in foraging for food and the relationship between shifting diets, diversifying

45 foraging strategies, and associated morphological specializations has yet to be outlined. In this
46 study we examine a group of mammals – the neotropical leaf-nosed bats – that occupy a distinct
47 yet impressively broad morphospace among bats while exhibiting unusually broad dietary
48 diversity (Freeman 2000; Dumont et al. 2012, 2014; Shi and Rabosky 2015; Hedrick et al. 2019),
49 in an attempt to test a model of ecological radiation in which sensory structure changes occur
50 before subsequent mechanical specialization.

51

52 The size of sensory structures in vertebrates is directly related to their functionality. In
53 fishes, birds, and mammals, larger eyes are related to greater visual acuity (Müller and Peichl
54 2005; Müller et al. 2007; Land and Nilsson 2012; Eklöf et al. 2014; Veilleux and Kirk 2014;
55 Sadier et al. 2018). Larger olfactory bulbs in at least mammals and birds support more expansive
56 epithelia and therefore larger surface areas for odor detection (Barton et al. 1995; Corfield et al.
57 2015). Finally, cochlear volume correlates with aspects of cochlear morphology that impact
58 hearing performance (Kirk and Gosselin-Ildari 2009; Kössl and Vater 2011; Vater and Kössl
59 2011). Mammals with derived echolocation capabilities have enlarged cochleae relative to their
60 body size (Kössl and Vater 1985; Davies et al. 2013a,b) while those that lack such capabilities
61 have much smaller cochleae relative to their size (Vater and Kössl 2011). Despite the apparent
62 relationship between sensory structures and food procurement , the evolutionary history of
63 sensory structures is poorly understood.

64 An ideal group to study the evolution of foraging and the evolution of sensory structures
65 would consist of closely related lineages that display drastically different foraging strategies and
66 diets. Noctilionoid bats (Superfamily Noctilionoidea) are a well-studied example of such dietary
67 disparity, collectively exhibiting more dietary strategies than any single mammalian order,

68 despite being a clade of only five closely related families. Among the five noctilionoid families
69 the Mormoopidae (ghost-faced, naked-backed, and mustached bats), Furipteridae, and
70 Thyropteridae are insectivorous, the Noctilionidae (bulldog bats) are insectivorous and
71 piscivorous, and the Mystacinidae (short-tailed bats) are generalists that consume insects,
72 flowers, and fruit. None of these families are particularly speciose though they contain notable
73 specializations such as *Mystacina tuberculata*'s crawling behavior and *Noctilio*'s ability to skim
74 fish out of water. Most of the dietary diversity within noctilionids lies within only one family,
75 Phyllostomidae (Neotropical leaf-nosed bats). The neotropical leaf nosed bats occupy the widest
76 diversity of dietary niches observed in vertebrates: nectar, pollen, fruit, foliage, birds, insects,
77 frogs, blood, and even other bats. Phyllostomids also are well known for their specialized skulls
78 and disparate hard-tissue morphologies (Dumont et al. 2014, Freeman 2000). As one family that
79 exhibits so many feeding strategies alongside well-known morphological disparity they are an
80 excellent starting place to trace the evolution of sensory structures related to foraging paralleling
81 mechanical adaptations to novel diets.

82 This study addresses the link between diet and sensory structures within the evolution of
83 noctilionoid bats using a well-supported phylogeny of the superfamily and a rich data set of
84 diceCT (diffusible iodine-based contrast-enhanced computed tomography) (Gignac and Kley
85 2014; Gignac et al. 2016) scans of bat specimens representing all dietary categories. However,
86 we removed the common vampire bat, *Desmodus rotundus*, from analyses as a dietary class with
87 a sample size of one would prevent statistical analyses. We use reconstructed soft tissue volumes
88 to examine variation in the relative sizes of sensory structures and to estimate ancestral states
89 throughout Noctilionoidea. Based on published studies of how these bats use olfactory, visual,
90 and auditory cues during foraging, we predict that, relative to their size, frugivores and

91 nectarivores evolved larger eyes and olfactory bulbs than animalivorous bats (piscivores,
92 insectivores, and carnivores), while animalivorous bats evolved larger cochlea than plant feeding
93 bats. We also expect that animalivorous bats evolved larger cochleae relative to the other sensory
94 organs, and that phytophagous bats evolved larger orbit and olfactory bulb volumes relative to
95 their cochleae. Because the phyllostomid ancestor was likely an insectivore that incorporated
96 plant matter into its diet (Freeman 2000; Baker et al. 2012), we expect to find enlarged orbits and
97 olfactory bulbs in the common ancestor of phyllostomids, but not in the common ancestors of
98 their sister-groups. Finally, given the novel cranial shape and corresponding dietary shift to
99 specialized frugivory within the phyllostomid subfamily stenodermatinae (Dumont et al. 2012;
100 Shi and Rabosky 2015), we expect corresponding shifts in the rates of evolution of eye and
101 olfactory bulb size at the base of this clade.

102

103 **Materials and Methods**

104

105 *Species representation and scan collection*

106 We measured the volumes of sensory tissues for 79 specimens representing 44 species of
107 the Neotropical Noctilionoideae and one outgroup species (*Mystacina tuberculata*) from the
108 mammal collections of the American Museum of Natural History and the University of
109 Massachusetts, Amherst. These species represent all of the major clades and dietary ecologies
110 except for the vampire bats. The specimens were fixed in 70% formalin and stored in ethanol for
111 varying time periods. All specimens were stained in a solution of Lugol's iodine (I₂KI) for two
112 weeks following Hedrick et al. (2018) before scanning them with a Nikon Metrology (X-Tek)

113 HTH 225 ST MicroCT scanner (Nikon Metrology Inc., Tokyo, Japan) at the Center for
114 Nanoscale Systems at Harvard University. Bats were scanned against a molybdenum target at
115 approximately 40 microns with voltage and current optimized for each scan (typically 70uA and
116 70kV). The resulting scans were then aligned in the proprietary CTPro software (CT Pro, Nikon
117 Metrology Inc., Tokyo, Japan) and slices were reconstructed in VG Studio Max (Volume
118 Graphics Inc., Germany).

119

120 *Soft Tissue Reconstruction and Adjusting for Head Size*

121 We imported the aligned scans into Mimics (Materialise, Leuven, Belgium – version 20)
122 and masked them to segment out the olfactory bulbs, eye orbits, and cochleae. For the olfactory
123 bulb, we masked the cavity demarcated by the cribriform plate and the imprint of the olfactory
124 bulb on the internal surface of the cranium. We were unable to separate the accessory olfactory
125 bulb from the primary olfactory bulb. For cochleae, we masked the hollow interior of the
126 complete bony labyrinth and we removed the vestibular system in GeoMagic Studio 2014
127 (3Dsystems, SC, USA). The preservation of museum specimens almost invariably shrinks the
128 eye itself (Hedrick et al., 2018). Therefore, we used the orbital space as defined by its muscular
129 boundaries and eyelid as a proxy for orbit size (see Hedrick et al., 2018 for details). We used
130 Mimics to measure volumes of the left and right orbits, olfactory bulbs, and cochleae for each
131 specimen, shown in figure 1. We averaged the volumes of tissues from the left and right of each
132 specimen and calculated species means for species for which we had more than one specimen.
133 As our goal is to understand the spatial relationships among the sensory organs within the
134 context of the skull, we used cranial centroid size as a proxy for head volume and used it to
135 adjust for head size. Centroid size is the sum of squared distances from the center of a cloud of

136 landmarks to each landmark and is proportional to the volume enclosed by the landmarks. To
137 ensure our results were not unjustly biased by skull length, centroid size was assessed in relation
138 to other metrics of skull size (skull length, width) as well (supporting materials). Centroid size
139 values were taken from Hedrick et al. (2019), which had cranial centroid sizes for all specimens
140 included in this analysis except *Dermanura phaeotis*. The centroid size of *D. phaeotis* was
141 substituted with the centroid size of *D. watsoni*, which is closely related and so similar in size
142 and morphology that they are difficult to distinguish

143

144 *Dietary Categories*

145 We grouped bat species into dietary categories following Rojas et al. (2018), who scored
146 the degree to which bat species rely on fruit, nectar, and insects/animals on an ordinal scale from
147 zero to three (no reliance to total reliance). We placed most species into the single dietary
148 category with the highest score. We categorized species with high scores in multiple food
149 sources as generalists (supporting materials).

150 *Comparative Analyses*

151 Comparative analyses were conducted using the tree generated by Rojas et al. (2016),
152 pruned to reflect the taxa represented in our sample. Phylogenetic regressions of \log_{10} sensory
153 structure volumes against \log_{10} centroid size were performed with the *phytools* function
154 *phyl.resid* in R (Revell 2012). These residuals represent the variance in sensory structure volume
155 that is not explained by centroid size and are treated as representative of sensory structure
156 volume for all subsequent analyses. Maximum likelihood estimates of lambda are built into the
157 regression function to account for phylogenetic signal of trait values. We used one-way

158 ANOVAs to determine whether the volumes of sensory structures varied among species within
159 different dietary categories, and Games-Howell *post hoc* tests to pinpoint differences between
160 categories. Spearman rank-order correlations were used to identify trends in size corresponding
161 to increased or decreased reliance on foods from each of the dietary categories.

162 Relative sensory investment for each specimen was quantified as the percentage of total
163 sensory volume represented by each sensory structure, and we compared sensory investment
164 across dietary categories using ANOVAs with Games-Howell *post hoc* tests. Because the bulk of
165 large-eyed frugivores are nested within one clade (Stenodermatinae), this clade might override
166 the signal coming from other frugivorous groups. For that reason, we first considered
167 stenodermatines grouped with the non-stenodermatine frugivores, then as a distinct group
168 separate from the non-stenodermatine frugivores.

169 *Ancestral Reconstructions and Shifts in Evolutionary Rates*

170 Ancestral states were inferred for \log_{10} size-adjusted volumes (volume/centroid) and \log_{10}
171 centroid size using the function *fastAnc* in the R package *phytools* (Revell 2012). We reverse log
172 transformed the resulting estimates and 95% confidence intervals following Thiagavel et al.
173 (2018) and then compared ancestral estimates and confidence intervals among the ancestors of
174 Phyllostomidae, Mormoopidae, Noctilionidae, and their most recent common ancestors. These
175 ancestral estimates were then compared with calculated averages and confidence intervals of
176 modern bats grouped by diet and family.

177 We used Bayesian Analysis of Macroevolutionary Mixtures (BAMM) v2.5 (Mitchell and
178 Rabosky 2017) in conjunction with the *BAMMtools* (Rabosky et al. 2014) and *coda* packages
179 (Plummer et al. 2006) in R to determine the plausibility of rate shifts in the evolution of centroid

180 size and size-adjusted volumes of sensory structures. For each analysis, the priors generated by
181 the package were used with 'expectedNumberOfShifts = 1' as recommended for small trees. The
182 Markov Chain Monte Carlo chains (MCMC) were run for ten million generations and sampled
183 every one thousand generations. MCMCs were checked for convergence after removing the first
184 10% as burn-in. Credible shift sets were generated for centroid size and each of the size adjusted
185 sensory volumes using a marginal odds ratio equal to 5.

186

187 **Results**

188 *Phylogenetic Regressions and Residuals*

189 The log₁₀ adjusted volumes of each of the three sensory structures correlated positively
190 with skull volume (olfactory $r_{(43)}=0.844$, $p<0.001$; orbit $r_{(43)}=0.799$, $p<0.001$; cochlea
191 $r_{(43)}=0.624$, $p<0.001$). Analysis of size-adjusted volumes (residuals from phylogenetic
192 regressions of sensory volumes against centroid size of the skull) reveal distinct trends in
193 olfactory bulb, orbit, and cochlea size among dietary categories. ANOVAs and *post hoc* tests
194 indicate that frugivores have the largest eyes and olfactory bulbs while nectarivores tend to have
195 small cochlea (Table 1). Frugivores occupy a distinct morphospace in orbit versus olfactory
196 volume residuals (Figure 2 a). All frugivores possess positive olfactory and orbit residuals while
197 most other bats have lower residual values on one or both axes. Nectarivores occupy a distinct
198 morphospace because of small cochlea volume residuals (Figure 2 b and c), though they have
199 moderate olfactory and orbit volume residuals.

200 We expected to find large eyes and olfactory bulbs among nectarivores but we did not.

201 Finding small cochlea among nectarivores was unexpected as well. To determine whether this

202 result (smaller than expected sensory sizes for all structures in nectarivores) was due to centroid
203 size overestimating skull size, we explored the relationship between centroid size and traditional
204 linear skull measurements. Centroid size of the skull correlates very well with skull length, but
205 overestimates skull width in nectarivorous bats. A phylogenetic regression of cochlea volume on
206 skull width yields the same result as the centroid size regression - nectarivorous bats have low
207 cochlea residuals. Because this finding holds even for the skull metric least represented by
208 centroid size, the result is unlikely to be caused by length-bias in centroid measurements
209 artificially distorting skull volume estimates in these species.

210 Spearman rank correlations indicate strong relationships between scores for dietary
211 reliance and sensory volume residuals. (Figure 3). The degree of animalivory is correlated
212 negatively with orbit ($r_{S(43)} = -0.540$, $p < 0.001$) and olfactory residuals ($r_{S(43)} = -0.509$, $p < 0.001$),
213 while degree of frugivory is positively correlated with both orbit ($r_{S(43)} = 0.613$, $p < 0.001$) and
214 olfactory residuals ($r_{S(43)} = 0.588$, $p < 0.001$). The degree of nectarivory is negatively correlated
215 with cochlea size ($r_{S(43)} = -0.582$, $p < 0.001$). There is no evidence of correlation between frugivory
216 and cochlea size, animalivory and cochlea size, nectarivory and olfactory size, or nectarivory and
217 orbit size.

218

219 *Sensory Proportions*

220 Overall, phyllostomid eyes and olfactory bulbs account for larger proportions of total
221 sensory volume compared to the other noctilionoid families, which feature larger proportions of
222 cochlear volume. ANOVAs comparing the relative proportions of sensory organs between
223 phyllostomids and outgroups (Figure 4) indicated that phyllostomid orbits account for a larger

224 proportion of their total sensory volume ($F_{(1,43)}=18.41$, $p<0.001$), cochleae account for a smaller
225 proportion ($F_{(1,43)}=138.46$, $p<0.001$), and olfactory bulbs account for a larger proportion
226 ($F_{(1,43)}=5.03$, $p=0.03$). Comparisons of sensory proportions among dietary groups within
227 Phyllostomidae showed moderate variation in the relative proportion of the cochlea ($F_{(3,31)}=3.45$,
228 $p=0.028$), more variation in the proportion of orbit ($F_{(3,31)}=4.15$, $p=0.014$), and little variation in
229 olfactory bulb proportion ($F_{(3,31)}=2.32$, $p=0.095$). Games-Howell *post hoc* tests indicate that the
230 significance in orbit proportion is accounted for primarily by the difference between
231 animalivores and nectarivores ($p=0.024$, $t=3.74$) and animalivores and frugivores ($p=0.013$,
232 $t=3.59$). When the stenodermatine bats are counted as their own dietary class within
233 Phyllostomidae, ANOVA and Games-Howell *post hoc* tests point to significant differences in
234 olfactory bulb proportion ($F_{(4,30)}=3.72$, $p=0.014$), with the stenodermatine frugivores having a
235 lower olfactory proportion than the other frugivores ($p=0.001$, $t=5.82$). In terms of proportion
236 accounted for by the orbit, variation among groups ($F_{(4,30)}=5.96$, $p=0.001$) is accounted for by the
237 difference between stenodermatines and other frugivores ($p=0.001$, $t=5.53$) and animalivores
238 ($p=0.005$, $t=4.38$), as well as the difference between nectarivores and non-stenodermatine
239 frugivores ($p=0.036$, $t=5.51$), and nectarivores and animalivores ($p=0.034$, $t=3.74$). ANOVAs for
240 cochlear volume proportions find significance when stenodermatine bats are treated alone
241 ($F_{(4,30)}=2.88$, $p=0.039$), but post-hoc tests do not detect notable variation among groups. Overall,
242 stenodermatines exhibit higher orbit and lower olfactory proportions than non-stenodermatine
243 frugivores. Non-stenodermatine frugivores have a lower proportion of orbit volume than
244 nectarivores in part because their olfactory bulbs are larger, not because their eyes are smaller.

245

246 *Ancestral State Estimation*

247 Ancestral state estimation yields an inferred ancestor for phyllostomids that is
248 considerably different from the ancestors of other noctilionoid families. In terms of centroid size,
249 the ancestor of modern phyllostomids had already begun to diverge towards a larger overall skull
250 volume (Figure 5 a). The phyllostomid ancestor also had relatively larger olfactory bulbs and
251 orbits than other ancestral nodes in the tree (Figure 5 b and c). The preservation of these
252 ancestral changes is maintained across all dietary groups within Phyllostomidae - even the
253 animalivores have larger olfactory bulbs, orbits, and centroid sizes than extant non-phyllostomid
254 noctilionoids. Frugivores have much larger eyes and olfactory bulbs than the predicted
255 phyllostomid ancestor. Modern nectarivores have diminished cochleae relative to the
256 phyllostomid ancestor and other dietary classes within Phyllostomidae (Figure 5 d). Frugivores,
257 generalists, and animalivores in the family have not diverged from each other substantially, or
258 from the phyllostomid ancestor in terms of cochlea size.

259

260 *BAMM and Evolution Rate Shifts*

261 BAMM analysis of centroid size and the volumes of sensory structures revealed an
262 unexpected suite of rate changes among noctilionoids and notable heterogeneity in the rate of
263 orbit evolution (Figure 6). The centroid posterior distribution has 31 configurations in its 95%
264 credible shift set. A one-shift configuration was most sampled at 37%, with the shift occurring in
265 the *Artibeus* lineage with a marginal odds ratio of 120.1. The zero-shift configuration was 4.9%
266 of the posterior. The 95% credible shift set for olfactory bulb volume contains four
267 configurations, and 86% of the posterior configurations have zero shifts. In contrast, the 95%
268 credible shift set for orbit contains 185 shift configurations, none of which predict a zero-shift
269 configuration. The two most sampled sets are a two-shift configuration and three-shift

270 configuration, each of which is only 12% of the posterior distribution. Both configurations
271 feature a shift at the base of the stenodermatine clade (marginal odds 205.5). The first
272 configuration has an additional shift at the base of the phyllostomine clade (marginal odds
273 138.3), while the second has two additional separate shifts within phyllostomines, one in the
274 lineage of *Chrotopterus auritus* (marginal odds 22.82) and the other in the lineage of
275 *Phyllostomus discolor* (marginal odds 30.08). Prior and posterior probabilities along with
276 marginal odds trees for each sensory structure and centroid size are included as supporting
277 materials. Zero-shift configurations have the most support for both cochlea and olfactory bulb
278 volumes while rate shifts are supported for orbit volume and centroid size. The 95% credible set
279 for the cochlear volume contains only three configurations, and 65% of the posterior
280 configurations have zero shifts.

281

282 **Discussion**

283 Estimating ancestral sensory structure volumes allows insight into the evolutionary
284 history of foraging and the transition into novel dietary niches. We found evidence that the
285 enlargement of visual and olfactory structures preceded the evolution of increased morphological
286 disparity associated with dietary diversification. This suggests that a step towards omnivory
287 could have been necessary before selection could act on morphological aspects of the skull
288 required for specialization for new food sources. In essence, animals need to be able to find new
289 foods for selective forces to be imposed by the new food resources. Our results also suggest that
290 sensory and mechanical systems have some degree of evolutionary autonomy. Although analyses
291 of the vertebrate skull are crucial for understanding the morphological underpinnings and
292 correlates of ecological diversification, they have focused predominantly on the links between

293 dietary ecology and skeletal traits (Felice et al. 2019; Soria-Barreto et al. 2019). Although food
294 consumption is a central role for the vertebrate skull, it is important to consider that the skull
295 harbors sensory components whose functions extend beyond mechanical demands to include
296 foraging (Conith et al. 2019), mating (Baum and Kelliher 2009), and communication (Brennan
297 and Zufall 2006, Arch and Narins 2008, Fleishman 1992).

298 We expected a shift in the rates of trait evolution at the base of the stenodermatine
299 subfamily coincident with the well-known shift in speciation rate within the Neotropical
300 noctilionoids (Dumont et al. 2012; Rojas et al. 2012; Shi and Rabosky 2015). Due to these bats'
301 reliance on figs, which signal ripeness with olfactory cues and possibly visual cues (Thies et al.
302 1998; Hodgkison et al. 2013), we expected shifts in the rate of orbit and olfactory bulb evolution
303 but no shifts in the rate of cochlea evolution. While a rate-shift in olfactory size is highly
304 improbable, a shift in the rate of orbit bulb evolution is likely. We expected only one shift in the
305 rate of evolution of orbit size at the base of stenodermatines but found support for several
306 possible shifts across frugivorous phyllostomids. However, certainty around any particular
307 configuration is low due to the heterogeneity in the rates of orbit evolution. Much like the
308 olfactory bulb, there are no detectable shifts in rate of evolution of cochlea size. The variability
309 in the rate of orbit evolution suggests that orbit size can respond quickly to dietary changes. In
310 contrast, the lack of rate shifts in olfactory size suggests that the olfactory bulb may be more
311 constrained and unable to evolve as rapidly (Yohe et al. 2020). It is also possible that radical
312 alterations in the size of the olfactory bulb from the ancestor were not needed to enter
313 phytophagous niches.

314 A frugivorous sensory morphotype notable for relatively large olfactory bulbs and orbits,
315 developed in parallel across multiple phyllostomid lineages that rely totally or partially on fruit.

316 The size of these sensory structures increases with the proportion of a bat's diet composed of
317 fruit and large orbits and olfactory bulbs evolved independently in at least three lineages where
318 fruit is an important resource. Bats that eat insects exclusively have markedly smaller olfactory
319 bulbs and orbits both within and outside of phyllostomids, indicating that the development of
320 enlarged structures used for visual and olfactory foraging is linked with diet and not just
321 ancestry. The presence of the frugivorous-like sensory morphotype – larger than expected
322 olfactory bulbs and orbits – in the ancestor of the phyllostomids indicates a shift toward
323 omnivory requiring foraging for fruits had already occurred at the base of the family.

324 Our results provide independent support for the proposition that the phyllostomid
325 ancestor incorporated plant matter into its diet (Freeman 2000; Santana and Dumont 2009; Baker
326 et al. 2012, Yohe et al. 2015) . In terms of sensory morphology, the divergence of the ancestor of
327 modern phyllostomids from its ancestors was characterized by increasing olfactory and orbit
328 volume, both of which are strongly correlated with increased frugivory (Figures 2, 4). The
329 ancestral shift to omnivory at the base of the phyllostomids left a lasting sensory imprint: the
330 pattern of relative sensory volume in animalivorous phyllostomids is more similar to that of
331 plant-eating phyllostomids than it is to those of other animalivorous noctilionoids, though the
332 absolute volumes are smaller. In addition, many predominantly animalivorous phyllostomids in
333 our data set occasionally eat fruit, which indicates their capacity to find and forage on plants.
334 Taken together, the phylogenetic data, comparative analyses of hard tissue, and comparative
335 analysis of soft tissue all provide strong evidence that the phyllostomid ancestor was
336 omnivorous, a flexible morphotype from which many dietary specializations evolved. From an
337 original state of specialization for aerial insectivory, ecological generalization by way of a shift

338 toward omnivory preceded rapid re-specialization into a myriad of dietary niches associated with
339 incredible morphological disparity.

340

341 Though the typical trend of generalists becoming specialists is supported by ecological
342 and evolutionary theory (Futuyma and Morena 1988, Schluter 2000), further research should be
343 directed at investigating transitions from reliance on a specific food resource to generalist
344 ecologies. Overall, our findings strengthen the case for coupling traditional studies of bony
345 structures with analyses of soft tissues and serve to highlight the role of sensory evolution in
346 ecological diversification. Our analysis of sensory systems in an evolutionary context offers new,
347 more nuanced insights into the evolutionary history of diet and foraging suggesting sensory
348 adaptations should precede biomechanical adaptations in cases where organisms would have to
349 be able to find new food resources in order to begin specializing for consumption of those food
350 resources.

351

352 **Literature Cited:**

353

354 Altenbach, J. S. 1989. Prey capture by the fishing bats *Noctilio leporinus* and *Myotis vivesi*.
355 *Journal of Mammalogy* 70:421–424. JSTOR.

356 Arch, V. S., & Narins, P. M. (2008). “Silent” signals: Selective forces acting on ultrasonic
357 communication systems in terrestrial vertebrates. *Animal behaviour*, 76(4), 1423.

358 Arnold, S. J. 2015. Morphology, Performance and Fitness I. *Integrative and Comparative*
359 *Biology* 23:347–361.

360 Baker, R. J., O. R. P. Bininda-Emonds, H. Mantilla-Meluk, C. A. Porter, and R. A. van den
361 Bussche. 2012. Molecular time scale of diversification of feeding strategy and morphology
362 in New World Leaf-Nosed Bats (Phyllostomidae): A phylogenetic perspective.
363 *Evolutionary History of Bats: Fossils, Molecules and Morphology* 385–409.

- 364 Barton, R. A., A. Purvis, and P. H. Harvey. 1995. Evolutionary radiation of visual and olfactory
365 brain systems in primates, bats and insectivores. *Philosophical Transactions of the Royal*
366 *Society B* 348.
- 367 Baum, M. J., and K. R. Kelliher. 2009. Complementary roles of the main and accessory olfactory
368 systems in mammalian mate recognition. *Annual Review of Physiology* 71:141–160.
369 *Annual Reviews*.
- 370 Bell, G. P., and M. B. Fenton. 1986. Visual acuity, sensitivity and binocularity in a gleaning
371 insectivorous bat, *Macrotus californicus* (Chiroptera: Phyllostomidae). *Animal Behaviour*
372 34:409–414.
- 373 Bhatnagar, K. P., and E. Meisami. 1998. Vomeronasal organ in bats and primates: extremes of
374 structural variability and its phylogenetic implications. *Microscopy Research and Technique*
375 43:465–475. Wiley Online Library.
- 376 Brennan, P. A., & Zufall, F. (2006). Pheromonal communication in
377 vertebrates. *Nature*, 444(7117), 308-315.
- 378 Buehlmann, C., Mangan, M. & Graham, P. 2020. Multimodal interactions in insect
379 navigation. *Anim Cogn* 23, 1129–1141
- 380 Conith, A. J., D. T. Lam, and R. C. Albertson. 2019. Muscle-induced loading as an important
381 source of variation in craniofacial skeletal shape. *genesis* 57:e23263. Wiley Online Library.
- 382 Corfield, J. R., Price, K., Iwaniuk, A. N., Gutiérrez-Ibáñez, C., Birkhead, T., & Wylie, D. R.
383 (2015). Diversity in olfactory bulb size in birds reflects allometry, ecology, and
384 phylogeny. *Frontiers in Neuroanatomy*, 9, 102.
- 385 Davies, K. T. J., P. J. J. Bates, I. Maryanto, J. A. Cotton, and S. J. Rossiter. 2013a. The Evolution
386 of Bat Vestibular Systems in the Face of Potential Antagonistic Selection Pressures for
387 Flight and Echolocation. *PLoS ONE* 8.
- 388 Davies, K. T. J., I. Maryanto, and S. J. Rossiter. 2013b. Evolutionary origins of ultrasonic
389 hearing and laryngeal echolocation in bats inferred from morphological analyses of the
390 inner ear. *Frontiers in Zoology*
- 391 Dumont, E. R., L. M. Dávalos, A. Goldberg, S. E. Santana, K. Rex, and C. C. Voigt. 2012.
392 Morphological innovation, diversification and invasion of a new adaptive zone. *Proceedings*
393 *of the Royal Society B: Biological Sciences* 279:1797–1805.
- 394 Dumont, E. R., I. R. Grosse, B. Baird, and L. M. Dávalos. 2014. Selection for mechanical
395 advantage underlies multiple cranial optima in New World Leaf-nosed bats. *Evolution*
396 68:1436–1449.
- 397 Eklöf, J., J. Šuba, G. Petersons, and J. Rydell. 2014. Visual acuity and eye size in five European
398 bat species in relation to foraging and migration strategies. *Environmental and Experimental*
399 *Biology*.

400 Felice, R. N., J. A. Tobias, A. L. Pigot, and A. Goswami. 2019. Dietary niche and the evolution
401 of cranial morphology in birds. *Proceedings of the Royal Society B* 286:20182677. The
402 Royal Society.

403 Fleishman, L. J. (1992). The influence of the sensory system and the environment on motion
404 patterns in the visual displays of anoline lizards and other vertebrates. *The American*
405 *Naturalist*, 139, S36-S61.

406 Freeman, P. W. 2000. *Mammalogy Papers : University of Nebraska Macroevolution in*
407 *Microchiroptera : Recoupling morphology and ecology with phylogeny Macroevolution in*
408 *Microchiroptera : Recoupling morphology and ecology with phylogeny. Evolutionary*
409 *Ecology.*

410 Freeman, P. W. 1995. Nectarivorous feeding mechanisms in bats. *Biological Journal of the*
411 *Linnean Society* 56:439–463.

412 Futuyma, D. J. and G. Moreno. 1988. The evolution of ecological specialization. *Annu. Rev.*
413 *Ecol. Evol.* 19:207 – 233.

414 Fyer, G., and T. D. Iles. 1972. Cichlid fishes of the great lakes of Africa.

415 Gignac, P. M., and N. J. Kley. 2014. Iodine-enhanced micro-CT imaging: Methodological
416 refinements for the study of the soft-tissue anatomy of post-embryonic vertebrates. *Journal*
417 *of Experimental Zoology Part B: Molecular and Developmental Evolution* 322:166–176.
418 Wiley Online Library.

419 Gignac, P. M., N. J. Kley, J. A. Clarke, M. W. Colbert, A. C. Morhardt, D. Cerio, I. N. Cost, P.
420 G. Cox, J. D. Daza, and C. M. Early. 2016. Diffusible iodine-based contrast-enhanced
421 computed tomography (diceCT): an emerging tool for rapid, high-resolution, 3-D imaging
422 of metazoan soft tissues. *Journal of anatomy* 228:889–909. Wiley Online Library.

423 Gonzalez-Terrazas, T. P., C. Martel, P. Milet-Pinheiro, M. Ayasse, E. K. V. Kalko, and M.
424 Tschapka. 2016. Finding flowers in the dark: Nectar-feeding bats integrate olfaction and
425 echolocation while foraging for nectar. *Royal Society Open Science* 3.

426 Grant, B. R., and P. R. Grant. 1993. Evolution of Darwin’s finches caused by a rare climatic
427 event. *Proceedings of the Royal Society of London. Series B: Biological Sciences* 251:111–
428 117. The Royal Society London.

429 Greenhall, A. M. 1972. The biting and feeding habits of the Vampire bat, *Desmodus rotundus*.
430 *Journal of Zoology* 168:451–461.

431 Hedrick, B. P., and E. R. Dumont. 2018. Putting the leaf-nosed bats in context: a geometric
432 morphometric analysis of three of the largest families of bats. *Journal of Mammalogy*
433 99:1042–1054. Oxford University Press US.

434 Hedrick, B. P., G. L. Mutumi, V. D. Munteanu, A. Sadier, K. T. J. Davies, S. J. Rossiter, K. E.
435 Sears, L. M. Dávalos, and E. Dumont. 2019. Morphological Diversification under High

436 Integration in a Hyper Diverse Mammal Clade. *Journal of Mammalian Evolution*, doi:
437 10.1007/s10914-019-09472-x.

438 Henze, M. J. and T. H. Oakley. 2015. The dynamic evolutionary history of pancrustacean eyes
439 and opsins. *Integ. Compar. Biology* 55:830-842. (10.1093/icb/icv100)

440 Herrel, A., and V. Holanova. 2008. Cranial morphology and bite force in Chamaeleolis lizards –
441 Adaptations to molluscivory? *Zoology* 111:467–475. Urban & Fischer.

442 Hodgkison, R., M. Ayasse, C. Häberlein, S. Schulz, A. Zubaid, W. A. W. Mustapha, T. H. Kunz,
443 and E. K. v Kalko. 2013. Fruit bats and bat fruits: the evolution of fruit scent in relation to
444 the foraging behaviour of bats in the New and Old World tropics. *Functional Ecology*
445 27:1075–1084. Wiley Online Library.

446 Jacobs, D. S., S. Catto, G. L. Mutumi, N. Finger, and P. W. Webala. 2017. Testing the sensory
447 drive hypothesis: geographic variation in echolocation frequencies of Geoffroy’s horseshoe
448 bat (*Rhinolophidae: Rhinolophus clivosus*). *PLoS One* 12. Public Library of Science.

449 Jones, G., and E. C. Teeling. 2006. The evolution of echolocation in bats. *Trends in Ecology &*
450 *Evolution* 21:149–156. Elsevier.

451 Kirk, E. C., and A. D. Gosselin-Ildari. 2009. Cochlear labyrinth volume and hearing abilities in
452 primates. *Anatomical Record* 292:765–776.

453 Kössl, M., and M. Vater. 2011. Cochlear Structure and Function in Bats.

454 Kössl, M., and M. Vater. 1985. Evoked acoustic emissions and cochlear microphonics in the
455 mustache bat, *Pteronotus parnellii*. *Hearing research* 19:157–170. Elsevier.

456 Land, M. F., and D.-E. Nilsson. 2012. *Animal eyes*. Oxford University Press.

457 Martin, J. P., Beyerlein, A., Dacks, A. M., Reisenman, C. E., Riffell, J. A., Lei, H., &
458 Hildebrand, J. G. 2011. The neurobiology of insect olfaction: sensory processing in a
459 comparative context. *Progress in neurobiology*, 95(3), 427-447. Mitchell, J.S. and Rabosky,
460 D.L., 2017. Bayesian model selection with BAMM: effects of the model prior on the
461 inferred number of diversification shifts. *Methods in Ecology and Evolution*, 8(1), pp.37-46.

462 Müller, B., S. M. Goodman, and L. Peichl. 2007. Cone photoreceptor diversity in the retinas of
463 fruit bats (*Megachiroptera*). *Brain, Behavior and Evolution* 70:90–104. Karger Publishers.

464 Müller, B., and L. Peichl. 2005. Retinal Cone Photoreceptors in Microchiropteran Bats.
465 *Investigative Ophthalmology and Visual Science* 46.

466 Nogueira, M. R., A. L. Peracchi, and L. R. Monteiro. 2009. Morphological correlates of bite
467 force and diet in the skull and mandible of phyllostomid bats. *Functional Ecology* 23:715–
468 723. Wiley Online Library.

469 Plummer, M., Best, N., Cowles, K. and Vines, K., 2006. CODA: convergence diagnosis and
470 output analysis for MCMC. *R news*, 6(1), pp.7-11.

471 Rabosky, D.L., Grundler, M., Anderson, C., Title, P., Shi, J.J., Brown, J.W., Huang, H. and
472 Larson, J.G., 2014. BAMM tools: an R package for the analysis of evolutionary dynamics
473 on phylogenetic trees. *Methods in Ecology and Evolution*, 5(7), pp.701-707.

474 Revell, L.J., 2012. phytools: an R package for phylogenetic comparative biology (and other
475 things). *Methods in Ecology and Evolution*, 3(2), pp.217-223.

476 Rojas, D., A. Vale, V. Ferrero, and L. Navarro. 2012. The role of frugivory in the diversification
477 of bats in the Neotropics. *Journal of Biogeography* 39:1948–1960. Wiley Online Library.

478 Sadier, A., K. T. J. Davies, L. R. Yohe, K. Yun, P. Donat, B. P. Hedrick, E. R. Dumont, L. M.
479 Davalos, S. J. Rossiter, and K. E. Sears. 2018. Multifactorial processes underlie parallel
480 opsin loss in neotropical bats. *Elife* 7:e37412. eLife Sciences Publications Limited.

481 Santana, S. E., and E. R. Dumont. 2009. Connecting behaviour and performance: The evolution
482 of biting behaviour and bite performance in bats. *Journal of Evolutionary Biology*, doi:
483 10.1111/j.1420-9101.2009.01827.x.

484 Santana, S. E., I. R. Grosse, and E. R. Dumont. 2012. Dietary hardness, loading behavior, and
485 the evolution of skull form in bats. *Evolution*, doi: 10.1111/j.1558-5646.2012.01615.x.

486 Schluter, D. 2000. *The Ecology of Adaptive Radiation*. OUP Oxford.

487 Schluter, D., and T. Price. 1997. Likelihood of Ancestor States in Adaptive Radiation.
488 *International Journal of Organic Evolution* 51.

489 Seehausen, O., Y. Terai, I. S. Megalhaes, K. L. Carleton, H. D. J. Mrosso, R. Miyagi, I. van der
490 Sluijs, M. v. Schneider, M. E. Maan, H. Tachida, H. Imai, and N. Okada. 2008. Speciation
491 through sensory drive in cichlid fish. *Nature* 455:620–626.

492 Shi, J., and D. Rabosky. 2015. Speciation dynamics during the global radiation of extant bats.
493 *Evolution* 69:1528–1545.

494 Soria-Barreto, M., R. Rodiles-Hernández, and K. O. Winemiller. 2019. Trophic ecomorphology
495 of cichlid fishes of Selva Lacandona, Usumacinta, Mexico. *Environmental Biology of*
496 *Fishes* 102:985–996. Springer.

497 Thiagavel, J., C. Cechetto, S. E. Santana, L. Jakobsen, E. J. Warrant, and J. M. Ratcliffe. 2018.
498 Auditory opportunity and visual constraint enabled the evolution of echolocation in bats.
499 *Nature Communications* 9. Springer US.

500 Thies, W., E. K. V. Kalko, and H. U. Schnitzler. 1998. The roles of echolocation and olfaction in
501 two Neotropical fruit-eating bats, *Carollia perspicillata* and *C. castanea*, feeding on *Piper*.
502 *Behavioral Ecology and Sociobiology* 42:397–409.

503 Vater, M., and M. Kössl. 2011. Comparative aspects of cochlear functional organization in
504 mammals. *Hearing Research* 273:89–99. Elsevier B.V.

505 Veilleux, C. C., and E. C. Kirk. 2014. Visual acuity in mammals: Effects of eye size and
506 ecology. *Brain, Behavior and Evolution* 83:43–53.

507 Yohe, L. R., R. Abubakar, C. Giordano, E. Dumont, K. E. Sears, S. J. Rossiter, and L. M.
 508 Dávalos. 2017. Trpc2 pseudogenization dynamics in bats reveal ancestral vomeronasal
 509 signaling, then pervasive loss. *Evolution* 71:923–935. Wiley Online Library.

510 Yohe, L.R., P.M. Velazco, D. Rojas, B. E. Gerstner, N. B. Simmons, L. M. Dávalos. 2015.
 511 Bayesian Hierarchical models suggest oldest known plant-visiting bat was omnivorous. *Biology*
 512 *Letters*, 11.11

513 Yohe, L. R., Davies, K. T., Simmons, N. B., Sears, K. E., Dumont, E. R., Rossiter, S. J., &
 514 Dávalos, L. M. (2020). Evaluating the performance of targeted sequence capture, RNA-Seq, and
 515 degenerate-primer PCR cloning for sequencing the largest mammalian multigene
 516 family. *Molecular Ecology Resources*, 20(1), 140-153.

517
 518
 519
 520
 521
 522
 523
 524
 525
 526

527 **Tables**

528 Table 1 a): Olfactory Residual Post Hoc Table

OB P values	Frugivore	Animalivore	Nectarivore	Generalist
Frugivore	XXX XXX	p=0.001, t=4.70	p=0.019, t=6.67	p=0.026, t=3.22
Animalivore		XXX XXX	p=0.975, t=0.41	p=0.213, t=2.01
Nectarivore			XXX XXX	p=0.093, t=2.91
Generalist				XXX XXX

529 ANOVA: $F_{(3,41)}=9.146$, $p<0.001$
 530 Games-Howell: $\eta^2=.4$, [.17;.52], $F=9.15$;

531

532 Table 1 b): Orbit Residual Post Hoc Table

Orb P values	Frugivore	Animalivore	Nectarivore	Generalist
Frugivore	XXX XXX	p<0.001, t=7.48	p=<0.001, t=6.01	p=0.001, t=4.56
Animalivore		XXX XXX	p=0.016, t=3.43	p=0.045, t=2.81
Nectarivore			XXX XXX	p=0.996, t=0.23
Generalist				XXX XXX

533 ANOVA: $F_{(3,41)}=9.146$, $p<0.001$

534 Games-Howell: $\eta^2=.61$, [.41;.69], $F=21.39$

535

536

537

538

539

540 Table 1 c) Cochlea Residual Post Hoc Table

Cochlea P values	Frugivore	Animalivore	Nectarivore	Generalist
Frugivore	XXX XXX	p=0.993, t=0.27	p=0.011, t=7.98	p=0.003, t=4.19
Animalivore		XXX XXX	p=0.002, t=5.22	p=0.094, t=2.45
Nectarivore			XXX XXX	p=0.049, t=3.52
Generalist				XXX XXX

541 ANOVA: $F_{(3,41)}=7.41$, $p<0.001$

542 Games-Howell: $\eta^2=.35$, [.12;.47], $F=7.41$

543

544 Table 1. Results of ANOVAs and subsequent post hoc tests performed on residuals of sensory
545 volumes regressed against centroid size. Values in bold text indicate that frugivores differ from
546 the other dietary classes in terms of orbit and olfactory size while nectarivores are unique with
547 respect to cochlea size.

548

549

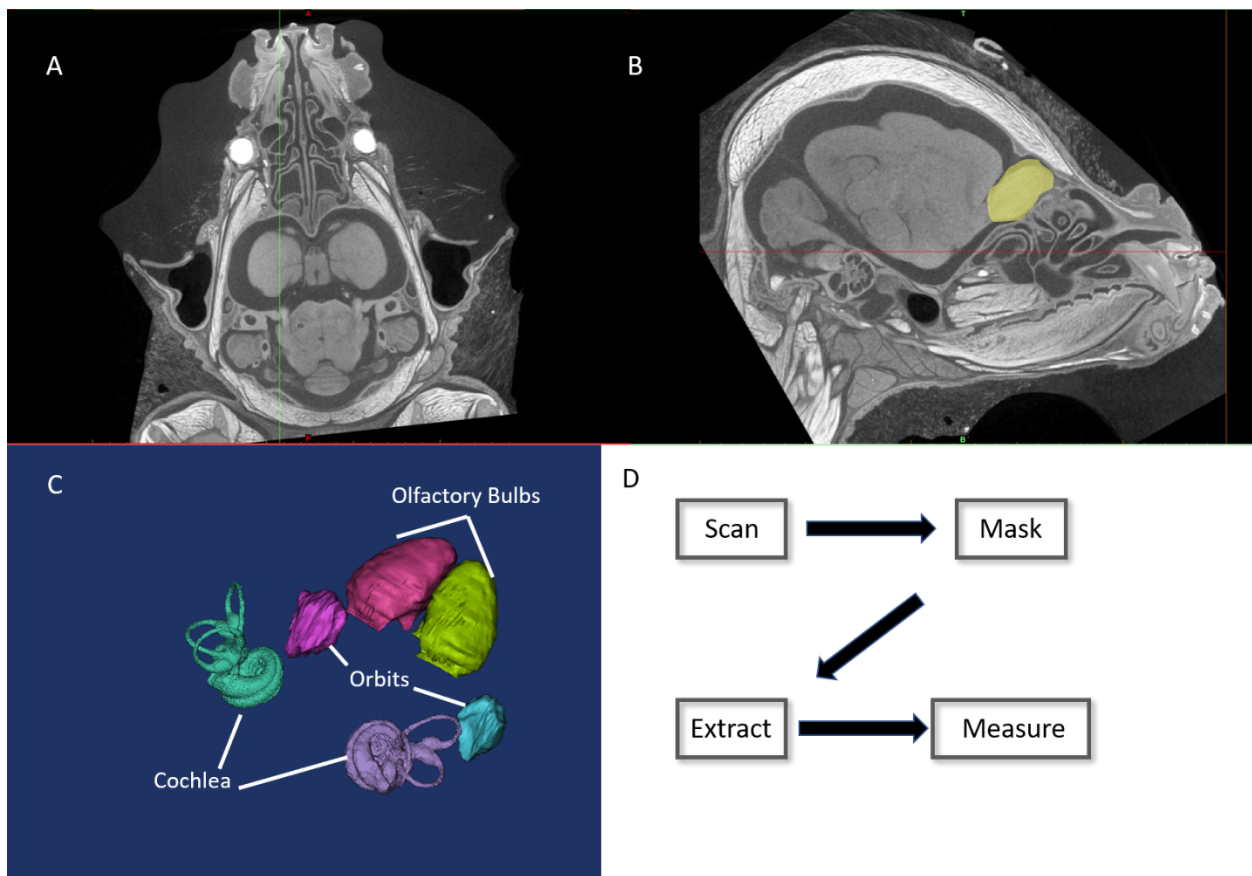
550

551

552 **Figures**

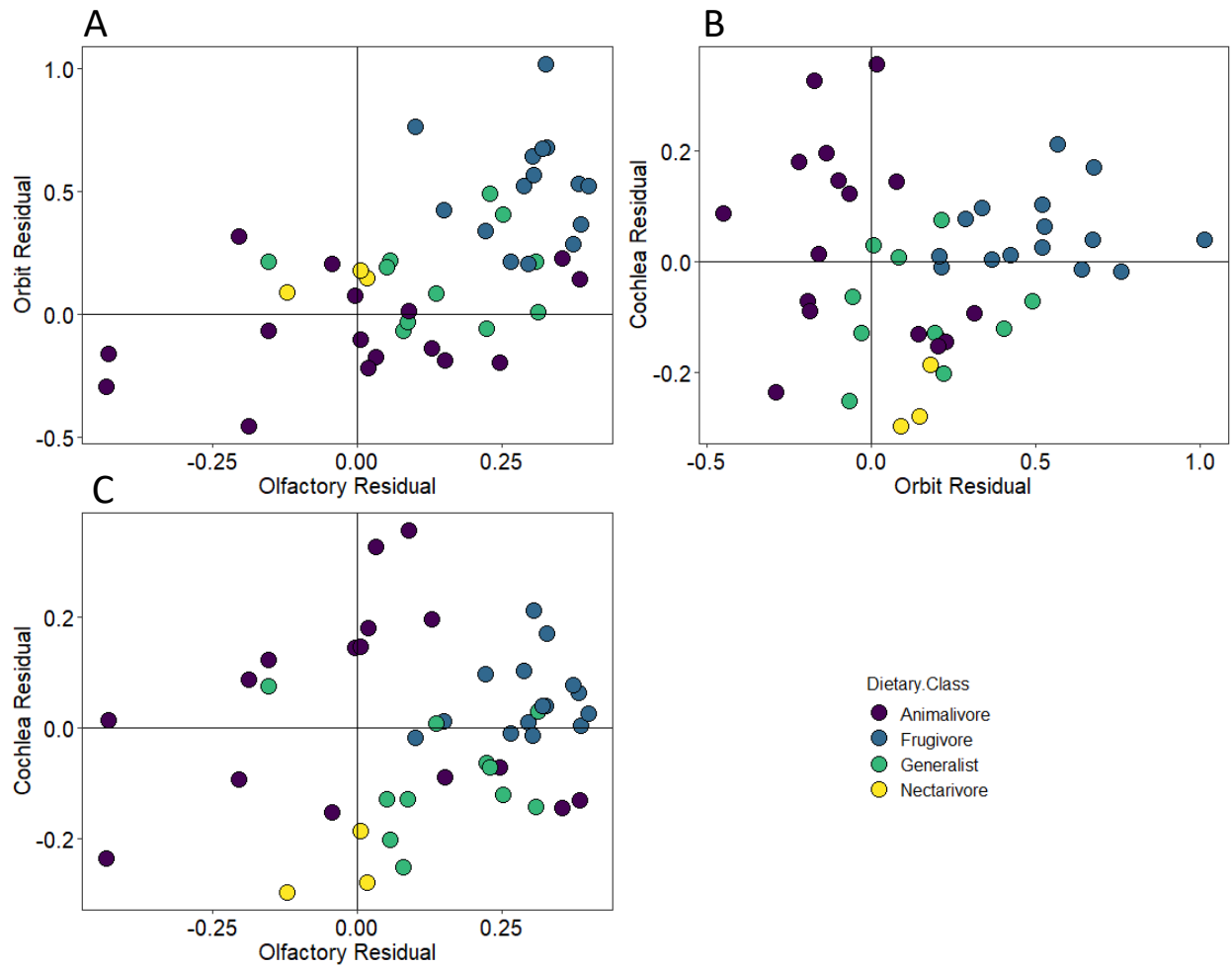
553

554 Figure 1



555

556 Figure 1: A) an axial cross section of a specimen, B) a sagittal cross section of the same bat
557 showing a slice of the olfactory mask, C) the structures extracted, D) the workflow resulting in
558 volumetric measurements. The software directly calculates the volumes of the shapes with no
559 additional manual measurements needing to be taken.



561

562 Figure 2. Plots of sensory structure residuals colored by diet: A) orbit residuals versus olfactory
563 residuals, all of the frugivores cluster in quadrant I; B) cochlea residuals against orbit residuals;
564 and C) cochlea residuals versus olfactory residuals.

565

566

567

568

569

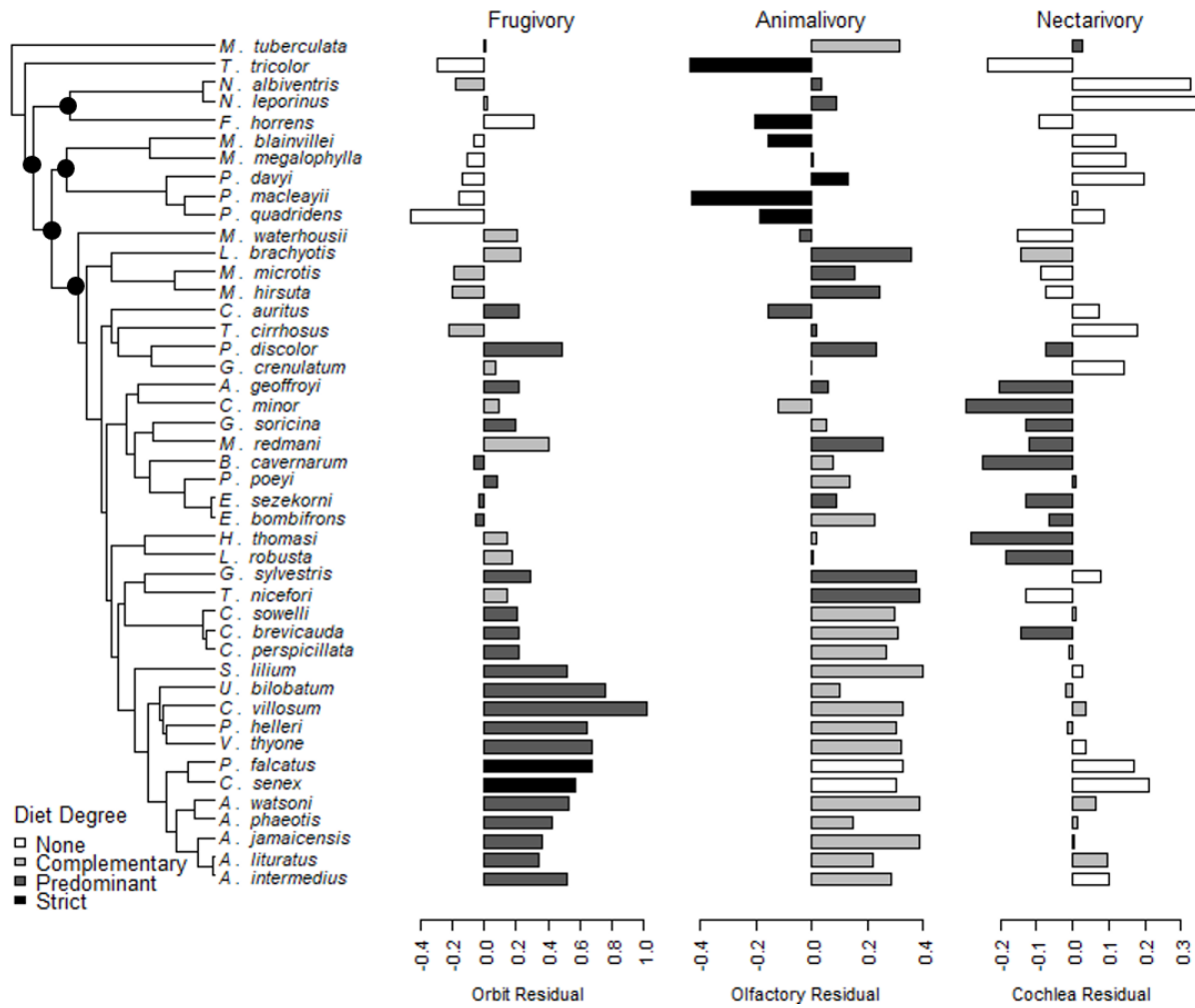
570

571

572

573

574 Figure 3



575

576

577 Figure 3. Residual values of orbit, olfactory bulb, and cochlea size for each species colored by
 578 whether the reliance on a specific diet is absent (none), complementary, predominant, or strict.
 579 Orbit residuals illustrate degree of frugivory, olfactory residuals are colored based on degree of
 580 animalivory, and cochlea is colored based on degree of nectarivory. Ancestral state
 581 reconstructions are provided for nodes highlighted in the tree in Fig 4.

582

583

584

585

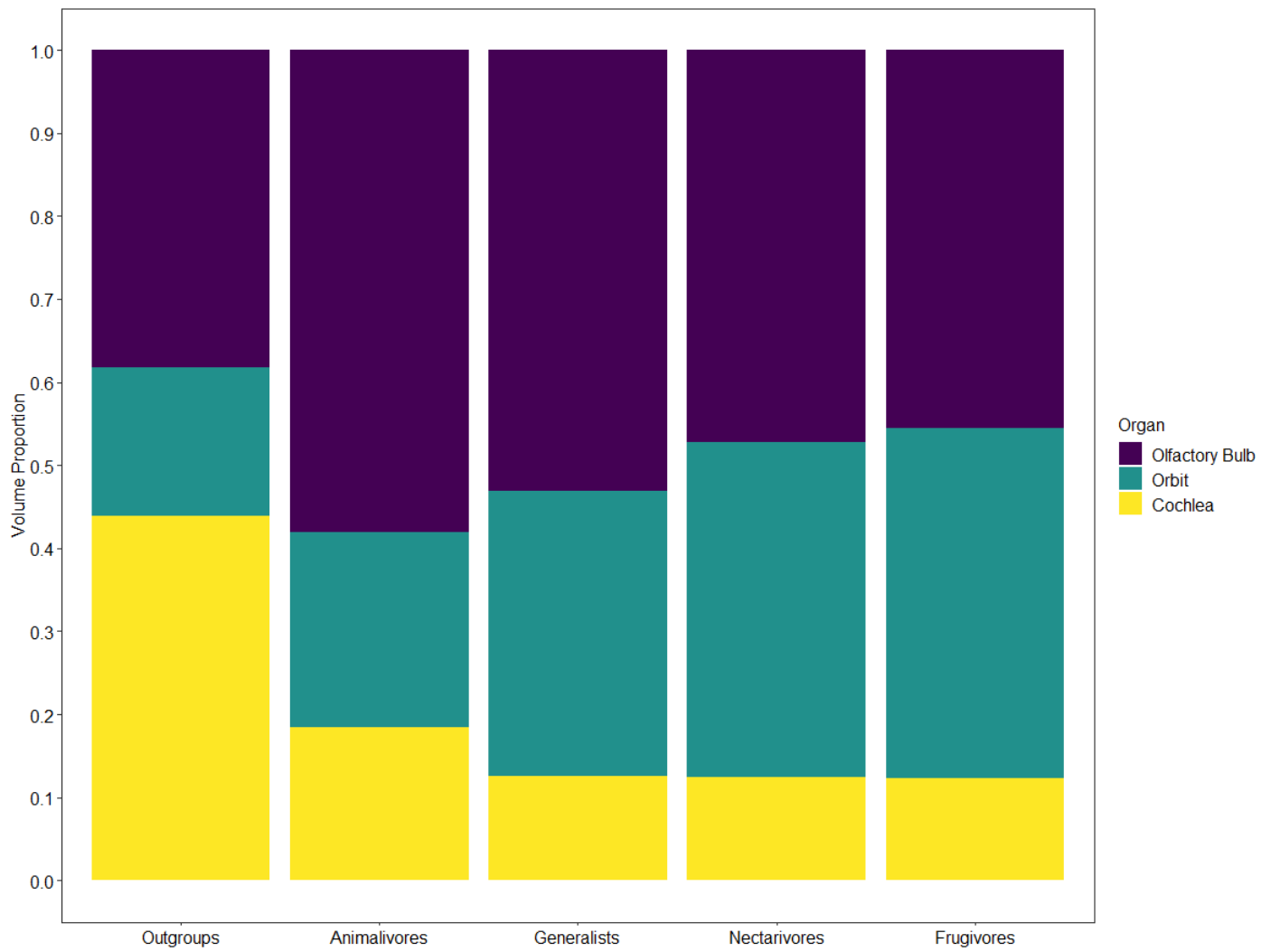
586

587

588

589 Figure 4

590



591

592

593 Figure 4. Average proportions of the olfactory bulb, orbit, and cochlea for non-phylostomids
594 (Outgroups) compared with the different dietary classes among phyllostomids.

595

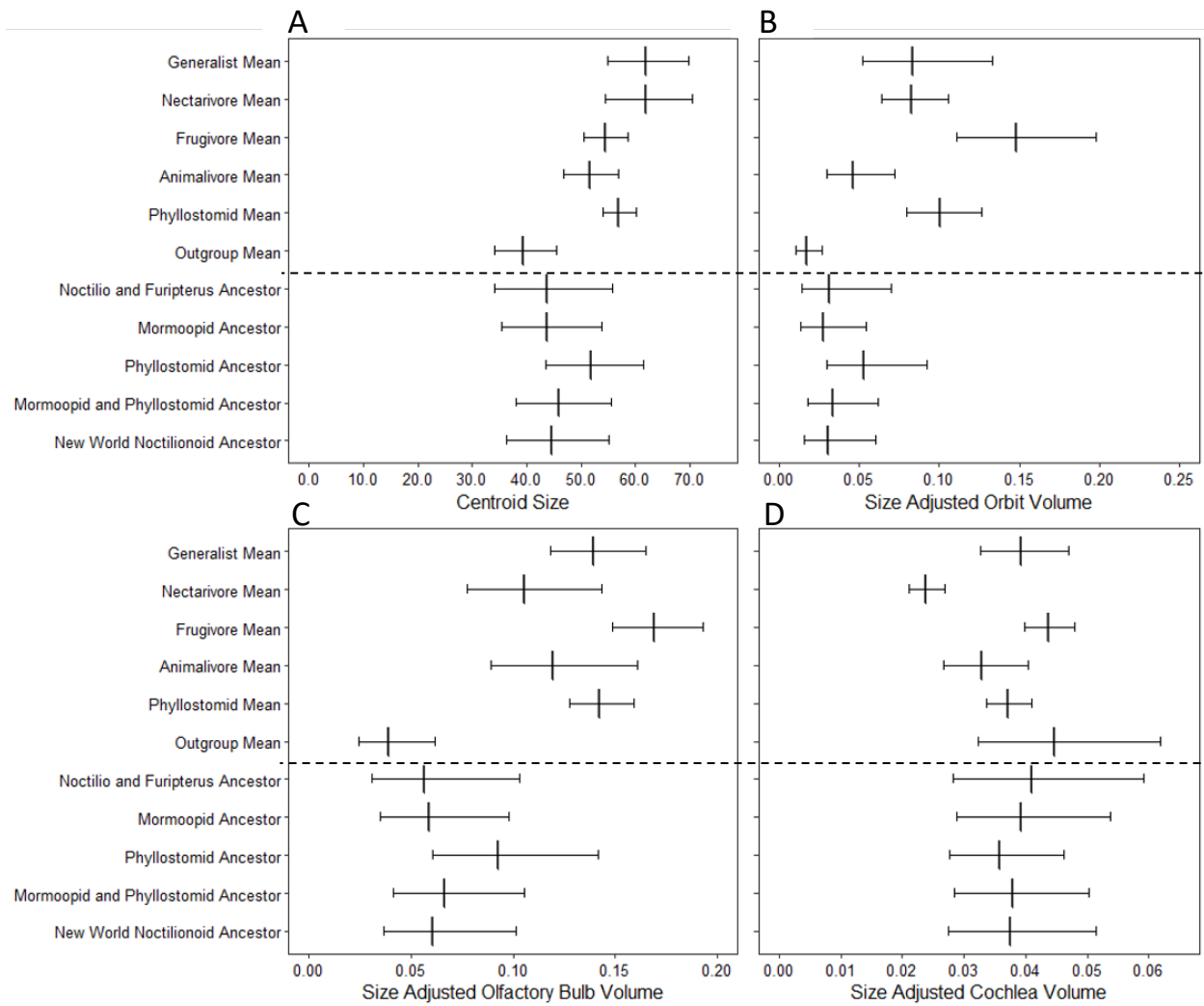
596

597

598

599

600



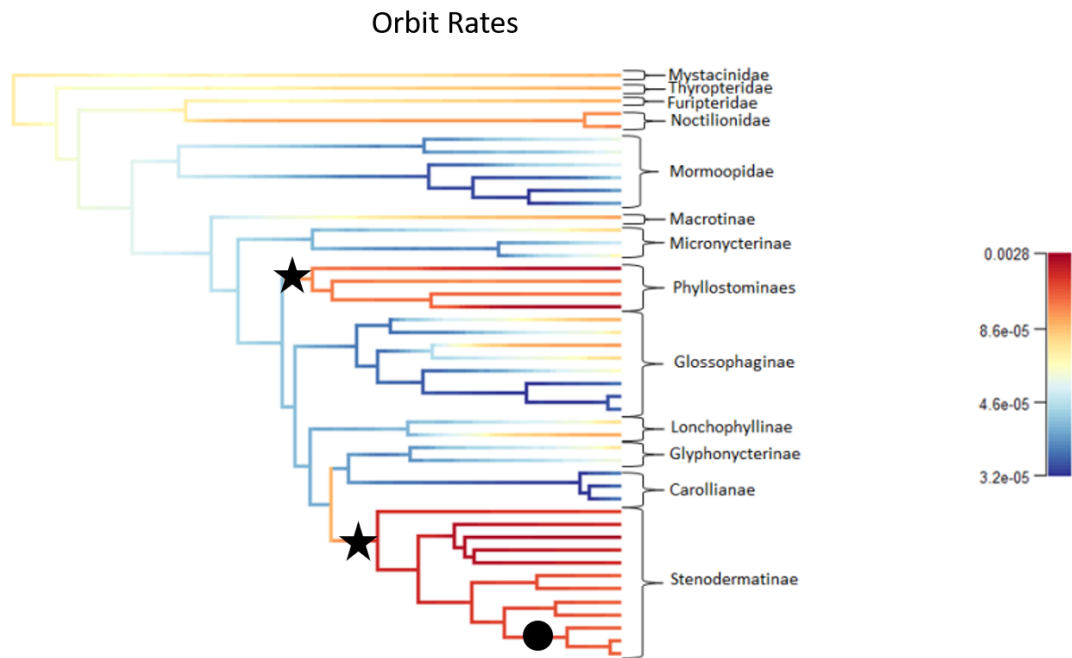
602

603 Figure 5. Ancestral state reconstructions for centroid size (A) and size-adjusted volumes of the
 604 orbit (B), olfactory bulb (C), and cochlea volumes (D). Ancestral nodes are marked in Figure 3.

605

606 Figure 6

607



608

609 Figure 6. Rate of evolution in orbit volume. Warm colors indicate faster rates and cool colors
610 indicate slower rates. Stars indicate locations of orbit shifts in the most probable rate-shift
611 configuration. The circle indicates the location of the centroid shift in the most probable rate-
612 shift configuration. Note that the difference between red and pale orange is two orders of
613 magnitude.